

k -Means Clustering for Persistent Homology

Yueqi Cao^{1,†}, Prudence Leung^{1,†}, and Anthea Monod^{1,†}

1 Department of Mathematics, Imperial College London, UK

† Corresponding e-mail: y.cao21@imperial.ac.uk

Abstract

Persistent homology is a methodology central to topological data analysis that extracts and summarizes the topological features within a dataset as a persistence diagram; it has recently gained much popularity from its myriad successful applications to many domains. However, its algebraic construction induces a metric space of persistence diagrams with a highly complex geometry. In this paper, we prove convergence of the k -means clustering algorithm on persistence diagram space and establish theoretical properties of the solution to the optimization problem in the Karush–Kuhn–Tucker framework. Additionally, we perform numerical experiments on various representations of persistent homology, including embeddings of persistence diagrams as well as diagrams themselves and their generalizations as persistence measures; we find that clustering performance directly on persistence diagrams and measures outperform their vectorized representations.

Keywords: Alexandrov geometry; Karush–Kuhn–Tucker optimization; k -means clustering; persistence diagrams; persistent homology.

1 Introduction

Topological data analysis (TDA) is a recently-emerged field of data science that applies algebraic topology to a wide range of data settings. A particular advantage of TDA is its flexibility and applicability both when there is a clear formalism to the data (e.g., rigorous metric space structure) and when there is less structure (e.g., networks and text). *Persistent homology* is a methodology from TDA that computes a stable statistical summary of data, capturing their “shape” and “size,” and has been implemented in many applications from a broad range of data-centric fields with great success. A major limitation of PH, however, is its output of a multiset of half-open intervals together with the set of zero-length intervals with infinite multiplicity, known as a *persistence diagram*. The algebraic topological construction of persistence diagrams results in a complex geometry which hinders their direct applicability to classical statistical and machine learning methods. In machine learning, a fundamental task is clustering, which groups observations of a similar nature to determine structure within the data. The k -means clustering algorithm is a fundamental clustering method.

In this paper, we study the k -means algorithm in persistence diagram space and establish its convergence. In particular, we provide a characterization of the solution to the optimization problem in the Karush–Kuhn–Tucker (KKT) framework and show that the solution is a partial optimal point, KKT point, as well as a local minimum. Experimentally, we study various representations of persistent homology in the k -means algorithm, as persistence diagram embeddings, on persistence diagrams themselves, as well as on their generalizations as persistence measures. To implement k -means clustering on persistence diagram and persistence measure space, we reinterpret the algorithm taking into account the appropriate metrics on these spaces as well as constructions of their respective means.

Related Work. Marchese *et al.* (2017) also study the k -means clustering in persistence diagram space and compare the performance to other machine learning classification algorithms; they also establishes local minimality of the solution to the optimization problem in the convergence of the algorithm. Our convergence study expands on the work of Marchese *et al.* (2017) to the more general KKT framework and differs experimentally by studying the performance of k -means clustering specifically in the context of persistent homology. Panagopoulos (2022) overviews clustering and TDA more generally, explaining how

topological concepts may apply to the problem of clustering. Other work studies topological data analytic clustering for time series data as well as space-time data (Islambekov & Gel, 2019; Majumdar & Laha, 2020).

The remainder of this paper is organized as follows. Section 2 provides the background on both persistent homology and k -means clustering. We give details on the various components of persistent homology needed to implement the k -means clustering algorithm. In Section 3, we provide main result on the convergence of the k -means algorithm in PD space in the KKT framework. Section 4 provides results to numerical experiments comparing the performance of k -means clustering on embedded persistence diagrams versus persistence diagrams and persistence measures. We close with a discussion on our contributions and ideas for future research in Section 5.

2 Background and Preliminaries

2.1 Persistent Homology

Persistent homology adapts homology from classical algebraic topology to data settings in a dynamic manner. Homology algebraically identifies and counts features of a general topological space that are invariant under continuous deformations, such as stretching and compressing. When considering the homology of a dataset as a finite topological space X , it is common to use simplicial homology over a field. This reduces a general topological space to a discretization as a union of simpler components glued together in a combinatorial fashion, which then makes efficient algorithms for homology computation directly applicable. These basic components are k -simplices, where each k -simplex is the convex hull of $k + 1$ affinely independent points x_0, x_1, \dots, x_k , denoted by $[x_0, x_1, \dots, x_k]$. A set constructed combinatorially of k -simplices is a *simplicial complex* K .

The dynamism of persistent homology is captured in the form of a *filtration*, which is a fundamental component of persistent homology and distinguishes it from classical homology. A filtration is a nested sequence of topological spaces, $X_0 \subseteq X_1 \subseteq \dots \subseteq X_n = X$. In this paper, we study *Vietoris–Rips* filtrations for finite metric spaces (X, d_X) , which are commonly used in applications and real-data settings. Let $\epsilon_1 \leq \epsilon_2 \leq \dots \leq \epsilon_n$ be an increasing sequence of parameters where each $\epsilon_i \in \mathbb{R}_{\geq 0}$. The *Vietoris–Rips complex* of X at scale ϵ_i $\text{VR}(X, \epsilon_i)$ is constructed by adding a node for each $x_j \in X$ and a k -simplex for each set $\{x_{j_1}, x_{j_2}, \dots, x_{j_{k+1}}\}$ with diameter $d(x_i, x_j)$ smaller than ϵ_i for all $0 \leq i, j \leq k$. We then obtain a Vietoris–Rips filtration

$$\text{VR}(X, \epsilon_1) \hookrightarrow \text{VR}(X, \epsilon_2) \hookrightarrow \dots \hookrightarrow \text{VR}(X, \epsilon_n),$$

where the sequence of inclusions induces maps in homology for any fixed dimension \bullet .

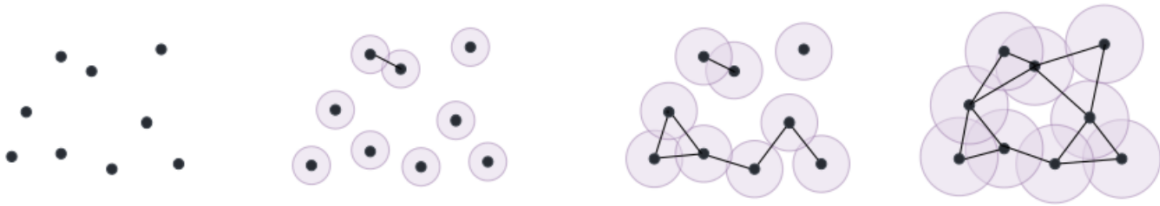


Figure 1: Example of a VR filtration and VR complexes at various increasing scales on a point cloud.

The sequence of inclusions induces maps in homology for any fixed dimension \bullet . Let $H_\bullet(X, \epsilon_i)$ be the homology group of $\text{VR}(X, \epsilon_i)$ with coefficients in a field. Then we have the following sequence of vector spaces:

$$H_\bullet(X, \epsilon_1) \rightarrow H_\bullet(X, \epsilon_2) \rightarrow \dots \rightarrow H_\bullet(X, \epsilon_n).$$

The collection of vector spaces $H_\bullet(X, \epsilon_i)$, together with vector space homomorphisms $H_\bullet(X, \epsilon_i) \rightarrow H_\bullet(X, \epsilon_j)$, is a *persistence module*.

For each finite dimensional $H_\bullet(X, \epsilon_i)$, the persistence module can be decomposed into rank one summands corresponding to birth and death times of homology classes (Chazal *et al.*, 2016): Let $\alpha \in H_\bullet(X, \epsilon_i)$ be a nontrivial homology class. α is *born* at ϵ_i if it is not in the image of $H_\bullet(X, \epsilon_{i-1}) \rightarrow H_\bullet(X, \epsilon_i)$ and similarly, it

dies entering ϵ_j if the image of α via $H_\bullet(X, \epsilon_i) \rightarrow H_\bullet(X, \epsilon_{j-1})$ is not in the image $H_\bullet(X, \epsilon_{i-1}) \rightarrow H_\bullet(X, \epsilon_{j-1})$, but the image of α via $H_\bullet(X, \epsilon_i) \rightarrow H_\bullet(X, \epsilon_j)$ is in the image $H_\bullet(X, \epsilon_{i-1}) \rightarrow H_\bullet(X, \epsilon_j)$. The collection of birth–death intervals $[\epsilon_i, \epsilon_j)$ represents the persistent homology of the Vietoris–Rips filtration of X . Taking each interval as an ordered pair of birth–death coordinates and plotting each in a plane \mathbb{R}^2 yields a persistence diagram; see Figure 2a.

Definition 1. A *persistence diagram* D is a locally finite multiset of points in the half-plane $\Omega = \{(x, y) \in \mathbb{R}^2 \mid x < y\}$ together with points on the diagonal $\partial\Omega = \{(x, x) \in \mathbb{R}^2\}$ counted with infinite multiplicity. Points in Ω are called *off-diagonal points*. The persistence diagram with no off-diagonal points is called the *empty persistence diagram*, denoted by D_\emptyset .

Intuitively, points that are far away from the diagonal are said to have *high persistence* and are generally considered to be topological signal, while points closer to the diagonal are considered to be topological noise.

A more general representation of persistence diagrams that aims to facilitate statistics and computations is the *persistence measure*. The construction of persistence measures arises from the equivalent representation of persistence diagrams as measures on Ω of the form $\sum_{x \in D \cap \Omega} n_x \delta_x$, where x ranges over the off-diagonal points in a persistence diagram D , n_x is the multiplicity of x , and δ_x is the Dirac measure at x Divol & Chazal (2019). Considering then all Radon measures supported on Ω gives the following definition.

Definition 2 (Divol & Lacombe (2021b)). Let μ be a Radon measure supported on Ω . For $1 \leq p < \infty$, the p -total persistence in this measure setting is defined as

$$\text{Pers}_p(\mu) = \int_{\Omega} \|x - x^\top\|_q^p d\mu(x),$$

where x^\top is the projection of x to the diagonal $\partial\Omega$. Any Radon measure with finite p -total persistence is called a *persistence measure*.

Persistence measures resemble heat map versions of persistence diagrams on the upper half-plane where individual persistence points are smoothed, so the intuition on their birth–death lifetimes are lost. However, they gain the advantage of a linear structure where statistical quantities are well-defined and much more straightforward to compute (Divol & Lacombe, 2021a).

Metrics for Persistent Homology. There exist several metrics for persistence diagrams; we focus on the following for its computational feasibility and the known geometric properties of persistence diagram space induced by this metric.

Definition 3. For $p > 0$, the p -Wasserstein distance between two persistence diagrams D_1 and D_2 is defined as

$$W_{p,q}(D_1, D_2) = \inf_{\gamma: D_1 \rightarrow D_2} \left(\sum_{x \in D_1} \|x - \gamma(x)\|_q^p \right)^{1/p},$$

where $\|\cdot\|_q$ denotes the q -norm, $1 \leq q \leq \infty$ and γ ranges over all bijections between D_1 and D_2 .

For a persistence diagram D , its p -total persistence is $W_{p,q}(D, D_\emptyset)$. We refer to the space of all persistence diagrams \mathcal{D}_p as the set of all persistence diagrams with finite p -total persistence. Equipped with the p -Wasserstein distance, $(\mathcal{D}_p, W_{p,q})$ is a well-defined metric space.

The space of persistence measures is equipped with the following metric.

Definition 4. The *optimal partial transport distance* between equivalent representation persistence measures μ and ν is

$$\text{OT}_{p,q}(\mu, \nu) = \inf_{\Pi} \left(\int_{\bar{\Omega} \times \bar{\Omega}} \|x - y\|_q^p d\Pi(x, y) \right)^{1/p},$$

with $\bar{\Omega} = \Omega \cup \partial\Omega$. Here, Π denotes the set of all Radon measures on $\bar{\Omega} \times \bar{\Omega}$ where for all Borel sets $A, B \subseteq \Omega$, $\Pi(A \times \bar{\Omega}) = \mu(A)$ and $\Pi(\bar{\Omega} \times B) = \nu(B)$.

The space of persistence measures \mathcal{M}_p , together with $\text{OT}_{p,q}$, is an extension and generalization of $(\mathcal{D}_p, W_{p,q})$. In particular, $(\mathcal{D}_p, W_{p,q})$ is a proper subset of $(\mathcal{M}_p, \text{OT}_{p,q})$ and $\text{OT}_{p,q}$ coincides with $W_{p,q}$ on the subset \mathcal{D}_p (Divol & Lacombe, 2021a).

2.2 k -Means Clustering

The k -means clustering algorithm is one of the most widely known unsupervised learning algorithms. It groups data points into k distinct clusters based on their similarities and without the need to provide any labels for the data (Hartigan & Wong, 1979). The process begins with a random sample of k points from the set of data points. Each data point is assigned to one of the k points, called *centroids*, based on minimum distance. Data points assigned to the same centroid form a *cluster*. The cluster centroid is updated to be the mean of the cluster. Cluster assignment and centroid update steps are repeated until convergence. The k -means algorithm is outlined fully in Algorithm 1.

Algorithm 1 k -Means Algorithm

Require: n data points (x_1, \dots, x_n) , fixed integer k , distance metric dist

- 1: **Initialization:** From (x_1, \dots, x_n) , randomly select k points as the initial centroids (m_1, \dots, m_k) .
- 2: **Assignment:** Assign each data point x_i to cluster k^* based on distance to each of the k centroids:

$$k^* = \operatorname{argmin}_k \text{dist}(x_i, m_k)$$

- 3: **Update:** Recompute cluster centroids m_k as the mean of the data points belonging to each cluster.

Repeat assignment and update steps until cluster assignment does not change, i.e., the algorithm converges.

A significant disadvantage of the k -means algorithm is that the final clustering output is highly dependent on the initial choice of k centroids. If initial centroids are close in terms of distance, this may result in suboptimal partitioning of the data. Therefore when using the k -means algorithm, it is preferable to begin with centroids that are as far from each other as possible such that they already lie in different clusters, which makes it more likely for convergence to the global optimum rather than a local solution. k -means++ (Arthur & Vassilvitskii, 2006) is an initialization algorithm that addresses this issue which we adapt in our implementation of the k -means algorithm, in place of the original random initialization step.

The original k -means algorithm presented by Hartigan & Wong (1979) takes vectors as input and calculates the squared Euclidean distance as the distance metric in the cluster assignment step. We adapt these inputs for the three embeddings of persistence diagrams outlined previously. For persistence diagrams and persistence measures, we adapt the algorithm to intake the p -Wasserstein distance $W_{p,q}$ and optimal partial transport distance $\text{OT}_{p,q}$, respectively.

2.3 Means for Persistent Homology

The existence of a mean and the ability to compute it is fundamental in the k -means algorithm. This quantity and its computation are nontrivial in persistence diagram space. A previously proposed notion of means for sets of persistence diagrams is based on Frchet means—generalizations of means to arbitrary metric spaces—where the metric is the p -Wasserstein distance (Turner *et al.*, 2014).

Specifically, given a set of persistence diagrams $\mathbf{D} = \{D_1, \dots, D_N\}$, define an empirical probability measure $\hat{\rho} = \frac{1}{N} \sum_{i=1}^N \delta_{D_i}$. The *Fréchet function* for any persistence diagram $D \in \mathbf{D}$ is then

$$F_{\hat{\rho}}(D) = \frac{1}{N} \sum_{i=1}^N W_{p,p}(D, D_i).$$

Since any persistence diagram D that minimizes the Fréchet function is the Fréchet mean of the set \mathbf{D} , the Fréchet mean in general need not be unique. This is the case in $(\mathcal{D}_2, W_{2,2})$, which is known to be an Alexandrov space with curvature bounded from below, meaning that geodesics and therefore Fréchet means are not even locally unique (Turner *et al.*, 2014). We will focus on the 2-Wasserstein distance in what follows and we use the notation W_2 for short. Nevertheless, they are computable as local minima, using a greedy algorithm that is a variant of the Hungarian algorithm, but have caveats: the Fréchet function is not convex

on \mathcal{D}_2 , which means the algorithm often finds only local minima; additionally, there is no initialization rule and arbitrary persistence diagrams are chosen as starting points, meaning that different initializations lead to an unstable performance and potentially different local minima.

For a set of persistence measures $\{\mu_1, \dots, \mu_N\}$, their mean is the *mean persistence measure*, which is simply the empirical mean of the set: $\bar{\mu} = \frac{1}{N} \sum_{i=1}^N \mu_i$.

3 Convergence of the k -Means Clustering Algorithm

Marchese *et al.* (2017) establish local minimality of the solution to the optimization problem in studying the convergence of the k -means algorithm. Here, we further investigate the various facets of the optimization problem in a Karush–Kuhn–Tucker framework and study and derive properties of the solution taking into account the subtleties and refinements of the Karush–Kuhn–Tucker setting. We focus on the 2-Wasserstein distance W_2 as in Section 2.3.

Problem Setup. Let $\mathbf{D} = \{D_1, \dots, D_n\}$ be a set of n persistence diagrams and let $\mathbf{G} = \{G_1, \dots, G_k\}$ be a partition of \mathbf{D} , i.e., $G_i \cap G_j = \emptyset$ for $i \neq j$ and $\cup_{i=1}^k G_i = \mathbf{D}$. Let $\mathbf{Z} = \{Z_1, \dots, Z_k\}$ be k persistence diagrams representing the centroids of a clustering. The within-cluster sum of distances is defined as

$$\mathbf{F}(\mathbf{G}, \mathbf{Z}) = \sum_{i=1}^k \sum_{D_j \in G_i} W_2^2(D_j, Z_i). \quad (1)$$

Define a $k \times n$ matrix $\omega = [\omega_{ij}]$ by setting $\omega_{ij} = 1$ if $D_j \in G_i$ and 0 otherwise. Then (1) can be equivalently expressed as

$$\mathbf{F}(\omega, \mathbf{Z}) = \sum_{i=1}^k \sum_{j=1}^n \omega_{ij} W_2^2(D_j, Z_i).$$

We first define a domain for each centroid Z_i : Let ℓ_i be the number of off-diagonal points of D_i ; let V be the convex hull of all off-diagonal points in $\cup_{i=1}^n D_i$. Define \mathbf{S} to be the set of persistence diagrams with at most $\sum_{i=1}^n \ell_i$ off-diagonal points in V ; the set \mathbf{S} is relatively compact (Mileyko *et al.*, 2011, Theorem 21).

Our primal optimization problem is

$$\begin{aligned} \min \quad & \mathbf{F}(\omega, \mathbf{Z}) \\ \text{s.t.} \quad & \begin{cases} \sum_{i=1}^k \omega_{ij} = 1 & \forall j = 1, \dots, n \\ \omega_{ij} = 0 \text{ or } 1 \\ Z_i \in \mathbf{S} & \forall i = 1, \dots, k. \end{cases} \end{aligned} \quad (\mathbf{P}_0)$$

We relax the integer constraints in optimization (\mathbf{P}_0) to continuous constraints by setting $\omega_{ij} \in [0, 1]$. Let Θ be the set of all $k \times n$ column stochastic matrices, i.e.,

$$\Theta = \{\omega \in \mathbb{R}^{k \times n} \mid \omega_{ij} \geq 0, \text{ and } \sum_i \omega_{ij} = 1 \forall j\}.$$

The relaxed optimization problem is then

$$\min \quad \mathbf{F}(\omega, \mathbf{Z}) \quad \text{s.t.} \quad \omega \in \Theta, \mathbf{Z} \in \mathbf{S}^k. \quad (\mathbf{P})$$

Finally, we reduce $\mathbf{F}(\omega, \mathbf{Z})$ to a univariate function $f(\omega) = \min\{\mathbf{F}(\omega, \mathbf{Z}), \mathbf{Z} \in \mathbf{S}^k\}$ by minimizing over the second variable. The reduced optimization problem is

$$\min \quad f(\omega) \quad \text{s.t.} \quad \omega \in \Theta. \quad (\mathbf{RP})$$

Lemma 5. *The optimization problems (\mathbf{P}_0) , (\mathbf{P}) , and (\mathbf{RP}) are equivalent.*

Proof. Problems (\mathbf{P}) and (\mathbf{RP}) are equivalent as they have the same constraints and equal cost functions. It suffices to prove (\mathbf{RP}) and the primal problem (\mathbf{P}_0) are equivalent.

Claim 1: $f(w)$ is a concave function on the convex set Θ .

Let $\omega_1, \omega_2 \in \Theta$, and $\lambda \in [0, 1]$. Set $\omega_\lambda = \lambda\omega_1 + (1 - \lambda)\omega_2$. Note that $\sum_i (\omega_\lambda)_{ij} = \lambda \sum_i (\omega_1)_{ij} + (1 - \lambda) \sum_i (\omega_2)_{ij} = 1$. Thus $\omega_\lambda \in \Theta$. Furthermore,

$$\begin{aligned} f(\omega_\lambda) &= \min_{\mathbf{Z}} \{\mathbf{F}(\omega_\lambda, \mathbf{Z})\} \\ &= \min_{\mathbf{Z}} \{\lambda \mathbf{F}(\omega_1, \mathbf{Z}) + (1 - \lambda) \mathbf{F}(\omega_2, \mathbf{Z})\} \\ &\geq \lambda \min_{\mathbf{Z}} \{\mathbf{F}(\omega_1, \mathbf{Z})\} + (1 - \lambda) \min_{\mathbf{Z}} \{\mathbf{F}(\omega_2, \mathbf{Z})\} \\ &= \lambda f(\omega_1) + (1 - \lambda) f(\omega_2). \end{aligned}$$

As a consequence, $f(w)$ always attains its minimum on the extreme points of Θ ; note that an extreme point is a point that cannot lie within the open interval of the convex combination of any two points.

Claim 2: The extreme points of Θ satisfy the constraints in (\mathbf{P}_0) .

The extreme points of Θ are 0-1 matrices which have exactly one 1 in each column (Cao *et al.*, 2022). They are precisely the constraints in (\mathbf{P}_0) .

In summary, any optimal point for (\mathbf{RP}) is also an optimal point for (\mathbf{P}_0) and vice versa. Thus, all three optimization problems are equivalent. \square

3.1 Convergence to Partial Optimal Points

We prove that Algorithm 1 for persistence diagrams always converges to partial optimal points in a finite number of steps. The proof is an extension of Theorem 3.2 by Marchese *et al.* (2017).

Definition 6. A point $(\omega_\star, \mathbf{Z}_\star)$ is a *partial optimal point* of (\mathbf{P}) if

- (i) $\mathbf{F}(\omega_\star, \mathbf{Z}_\star) \leq \mathbf{F}(\omega, \mathbf{Z}_\star)$ for all $\omega \in \Theta$, i.e., ω_\star is a minimizer of the function $\mathbf{F}(\cdot, \mathbf{Z}_\star)$; and
- (ii) $\mathbf{F}(\omega_\star, \mathbf{Z}_\star) \leq \mathbf{F}(\omega_\star, \mathbf{Z})$ for all $\mathbf{Z} \in \mathcal{S}^k$, i.e., \mathbf{Z}_\star is a minimizer of the function $\mathbf{F}(\omega_\star, \cdot)$.

Theorem 7. (Marchese *et al.*, 2017, Theorem 3.2) *The k -means algorithm over (\mathcal{D}_2, W_2) converges to a partial optimal point in finitely many steps.*

Proof. The value of \mathbf{F} only changes at two steps during each iteration. Fix an iteration t and let $\mathbf{Z}^{(t)} = \{Z_1^{(t)}, \dots, Z_k^{(t)}\}$ be the k centroids from iteration t . At the first step of the $(t + 1)$ st iteration, since we are assigning all persistence diagrams to a closest centroid, for any datum D_j ,

$$\sum_{i=1}^k \omega_{ij}^{(t+1)} W_2^2(D_j, Z_i^{(t)}) = \min_i \{W_2^2(D_j, Z_i^{(t)})\} = \sum_{i=1}^k \omega_{ij}^{(t)} \min_i \{W_2^2(D_j, Z_i^{(t)})\} \leq \sum_{i=1}^k \omega_{ij}^{(t)} W_2^2(D_j, Z_i^{(t)}).$$

Summing over $j = 1, \dots, n$, we have $\mathbf{F}(\omega^{(t+1)}, \mathbf{Z}^{(t)}) \leq \mathbf{F}(\omega^{(t)}, \mathbf{Z}^{(t)})$.

At the second step of the $(t + 1)$ st iteration, by the definition of Fréchet means, we have

$$Z_i^{(t+1)} = \arg \min_{\mathbf{Z}} \sum_{j=1}^n \omega_{ij}^{(t+1)} W_2^2(D_j, \mathbf{Z}).$$

Thus

$$\sum_{j=1}^n \omega_{ij}^{(t+1)} W_2^2(D_j, Z_i^{(t+1)}) \leq \sum_{j=1}^n \omega_{ij}^{(t+1)} W_2^2(D_j, Z_i^{(t)}).$$

Summing over $i = 1, \dots, k$, we have $\mathbf{F}(\omega^{(t+1)}, \mathbf{Z}^{(t+1)}) \leq \mathbf{F}(\omega^{(t+1)}, \mathbf{Z}^{(t)})$.

In summary, the function $\mathbf{F}(\omega, \mathbf{Z})$ is nonincreasing at each iteration. Since there are only finitely many extreme points in Θ , the algorithm is stable at a point ω_\star after finitely many steps. If we fix one Fréchet mean \mathbf{Z}_\star for $\mathbf{F}(\omega_\star, \cdot)$, then $(\omega_\star, \mathbf{Z}_\star)$ is a partial optimal point for (\mathbf{P}) by construction. \square

Theorem 7 is a revision of the original statement in Marchese *et al.* (2017), since the algorithm may not converge to local minima of (\mathbf{P}) .

Note that $\mathbf{F}(\omega, \mathbf{Z})$ is differentiable as a function of ω but not differentiable as a function of \mathbf{Z} . However, given that we are restricting to (\mathcal{D}_2, W_2^2) , there is a differential structure and in particular, the square distance function admits gradients in the Alexandrov sense (Turner *et al.*, 2014).

Given a point $D \in \mathcal{D}_2$, let Σ_D be the set of all nontrivial unit-speed geodesics emanating from D . The angle between two geodesics γ_1, γ_2 is defined as

$$\angle_D(\gamma_1, \gamma_2) = \arccos \left(\lim_{s, t \rightarrow 0} \frac{s^2 + t^2 - W_2(\gamma_1(s), \gamma_2(t))}{2st} \right).$$

By identifying geodesics $\gamma_1 \sim \gamma_2$ with zero angles, we define the space of directions $(\widehat{\Sigma}_D, \angle_D)$ as the completion of Σ_D / \sim under the angular metric \angle_D . The tangent cone $T_D = \widehat{\Sigma}_D \times [0, \infty) / \widehat{\Sigma}_D \times \{0\}$ is the Euclidean cone over $\widehat{\Sigma}_D$ with the cone metric defined as

$$C_D([\gamma_1, t], [\gamma_2, s]) = s^2 + t^2 - 2st \cos \angle_D(\gamma_1, \gamma_2).$$

The inner product is defined as $\langle [\gamma_1, t], [\gamma_2, s] \rangle_D = st \cos \angle_D(\gamma_1, \gamma_2)$. Let $v = [\gamma, t] \in T_D$. For any function $h : \mathcal{P} \rightarrow \mathbb{R}$, the differential of h at a point D is a map $T_D \rightarrow \mathbb{R}$ defined by

$$d_D h(v) = \lim_{s \rightarrow 0} \frac{h(\gamma_v(s)) - h(D)}{s}$$

if the limit exists and is independent of selection of γ_v . The gradient of h at D is a tangent vector $\nabla_D h \in T_D$ such that (i) $d_D h(u) \leq \langle \nabla_D h, u \rangle_D$ for all $u \in T_D$; and (ii) $d_D h(\nabla_D h) = \langle \nabla_D h, \nabla_D h \rangle$. Let $Q_D(\cdot) = W_2^2(\cdot, D)$ be the squared distance to D .

Lemma 8. (Turner *et al.*, 2014)

1. Q_D is Lipschitz continuous on any bounded set;
2. The differential and gradient are well-defined for Q_D ;
3. If D' is a local minimum of Q_D then $\nabla_{D'} Q_D = 0$.

Since \mathbf{F} is a linear combination of squared distance functions, by Lemma 8, the gradient exists for any variable Z_i . Thus, we formally write the gradient of \mathbf{F} as $\nabla_{\mathbf{Z}} \mathbf{F} = (\nabla_{Z_1} \mathbf{F}, \dots, \nabla_{Z_k} \mathbf{F})$.

Following Selim & Ismail (1984), we define the Karush–Kuhn–Tucker points for (\mathbf{P}) as follows.

Definition 9. A point $(\omega_\bullet, \mathbf{Z}_\bullet)$ is a *Karush–Kuhn–Tucker (KKT) point* of (\mathbf{P}) if there exists $\mu_1, \dots, \mu_n \in \mathbb{R}$ such that

$$\begin{cases} \frac{\partial \mathbf{F}}{\partial \omega_j}(\omega_\bullet, \mathbf{Z}_\bullet) + \mu_j \mathbf{1} = 0 & \forall j = 1, \dots, n \\ \mathbf{1}^\top (\omega_\bullet)_j - 1 = 0 & \forall j = 1, \dots, n \\ \nabla_{\mathbf{Z}} \mathbf{F}(\omega_\bullet, \mathbf{Z}_\bullet) = 0 \end{cases}$$

where $\mathbf{1}$ is the all-1 vector.

Theorem 10. The partial optimal points of (\mathbf{P}) are Karush–Kuhn–Tucker points of (\mathbf{P}) .

Proof. Suppose $(\omega_\star, \mathbf{Z}_\star)$ is a partial optimal point. Since ω_\star is a minimizer of the function $\mathbf{F}(\cdot, \mathbf{Z}_\star)$, it satisfies the Karush–Kuhn–Tucker conditions of the constrained optimization problem

$$\min_{\omega} \mathbf{F}(\omega, \mathbf{Z}_\star) \quad \text{s.t.} \quad \omega \in \Theta$$

which are exactly the first two conditions of being a Karush–Kuhn–Tucker point. Similarly, since \mathbf{Z}_\star is a minimizer of the function $\mathbf{F}(\omega_\star, \cdot)$, by Lemma 8, the gradient vector is zero, which is the third condition of a Karush–Kuhn–Tucker point. Thus, $(\omega_\star, \mathbf{Z}_\star)$ is a Karush–Kuhn–Tucker point of (\mathbf{P}) . \square

Conversely, suppose (ω_*, \mathbf{Z}_*) is a Karush–Kuhn–Tucker point. Since $\mathbf{F}(\cdot, \mathbf{Z}_*)$ is a linear function of ω and $\omega \in \Theta$ is a linear constraint, the first two conditions are sufficient for ω_* to be a minimizer of $\mathbf{F}(\cdot, \mathbf{Z}_*)$. Thus ω_* satisfies the first condition of a partial optimal point. However, the condition $\nabla_{\mathbf{Z}} \mathbf{F}(\omega_*, \mathbf{Z}_*) = 0$ cannot guarantee that \mathbf{Z}_* satisfies the second condition of a partial optimal point. Note that the original proof in Selim & Ismail (1984) of Theorem 4 is also incomplete.

Moreover, being a partial optimal point or Karush–Kuhn–Tucker point is not sufficient for being a local minimizer of the original optimization problem. A counterexample can be found in Selim & Ismail (1984).

3.2 Convergence to Local Minima

We now give a characterization of the local minimality of ω using directional derivatives of the objective function $f(\omega)$ in (RP). For any fixed element $\omega_0 \in \Theta$, let $v \in \mathbb{R}^{kn}$ be a feasible direction, i.e., $\omega_0 + tv \in \Theta$ for small t . The directional derivative of $f(\omega)$ along v is defined as

$$Df(\omega_0; v) := \lim_{t \rightarrow 0^+} \frac{f(\omega_0 + tv) - f(\omega_0)}{t},$$

if the limit exists. Let $\mathcal{Z}(\omega_0)$ be the set of all \mathbf{Z} minimizing the function $\mathbf{F}(\omega_0, \cdot)$. We have the following explicit formula for the directional derivatives of $f(\omega)$.

Lemma 11. *For any $\omega_0 \in \Theta$ and any feasible direction v , the directional derivative $Df(\omega_0; v)$ exists, and*

$$Df(\omega_0; v) = \min_{\mathbf{Z} \in \mathcal{Z}(\omega_0)} \left\{ \sum_{i=1}^k \sum_{j=1}^n v_{ij} W_2^2(D_j, Z_i) \right\}.$$

Proof. Denote

$$L(\omega_0; v) := \min_{\mathbf{Z} \in \mathcal{Z}(\omega_0)} \left\{ \sum_{i=1}^k \sum_{j=1}^n v_{ij} W_2^2(D_j, Z_i) \right\}.$$

For any $\mathbf{Z}_* \in \mathcal{Z}(\omega_0)$, we have

$$\begin{aligned} \frac{f(\omega_0 + tv) - f(\omega_0)}{t} &= \frac{\min_{\mathbf{Z} \in \mathbf{S}^k} \{\mathbf{F}(\omega_0 + tv, \mathbf{Z})\} - \min_{\mathbf{Z} \in \mathbf{S}^k} \{\mathbf{F}(\omega_0, \mathbf{Z})\}}{t} \\ &\leq \frac{\mathbf{F}(\omega_0 + tv, \mathbf{Z}_*) - \mathbf{F}(\omega_0, \mathbf{Z}_*)}{t} = \sum_{i=1}^k \sum_{j=1}^n v_{ij} W_2^2(D_j, Z_i). \end{aligned}$$

Thus we have

$$\limsup_{t \rightarrow 0^+} \frac{f(\omega_0 + tv) - f(\omega_0)}{t} \leq L(\omega_0; v). \quad (2)$$

It suffices to prove

$$\liminf_{t \rightarrow 0^+} \frac{f(\omega_0 + tv) - f(\omega_0)}{t} \geq L(\omega_0; v).$$

To do this, let t_j be a sequence tending to 0 and

$$\frac{f(\omega_0 + t_j v) - f(\omega_0)}{t_j} \rightarrow \liminf_{t \rightarrow 0^+} \frac{f(\omega_0 + tv) - f(\omega_0)}{t}$$

as $j \rightarrow \infty$. Choose $\mathbf{Z}_j \in \mathcal{Z}(\omega_0 + t_j v)$ for each j . Since \mathbf{S}^k is relatively compact, there is a subsequence of $\{\mathbf{Z}_j\}$ converging to some point \mathbf{Z}_* . We still denote the subsequence by $\{\mathbf{Z}_j\}$ for the sake of convenience. By Lemma 8, $\mathbf{F}(\omega, \mathbf{Z})$ is continuous. Thus, for any $\mathbf{Z} \in \mathbf{S}^k$,

$$\mathbf{F}(\omega_0, \mathbf{Z}_*) = \lim_{j \rightarrow \infty} \mathbf{F}(\omega_0 + t_j v, \mathbf{Z}_j) \leq \lim_{j \rightarrow \infty} \mathbf{F}(\omega_0 + t_j v, \mathbf{Z}) = \mathbf{F}(\omega_0, \mathbf{Z}).$$

That is, $\mathbf{Z}_\star \in \mathcal{Z}(\omega_0)$. Therefore, we have

$$\begin{aligned}
\liminf_{t \rightarrow 0^+} \frac{f(\omega_0 + tv) - f(\omega_0)}{t} &= \lim_{j \rightarrow \infty} \frac{\mathbf{F}(\omega_0 + t_j v, \mathbf{Z}_j) - \mathbf{F}(\omega_0, \mathbf{Z}_\star)}{t_j} \\
&= \lim_{j \rightarrow \infty} \frac{\mathbf{F}(\omega_0 + t_j v, \mathbf{Z}_j) - \mathbf{F}(\omega_0, \mathbf{Z}_j)}{t_j} + \lim_{j \rightarrow \infty} \frac{\mathbf{F}(\omega_0, \mathbf{Z}_j) - \mathbf{F}(\omega_0, \mathbf{Z}_\star)}{t_j} \\
&\geq \lim_{j \rightarrow \infty} \frac{\mathbf{F}(\omega_0 + t_j v, \mathbf{Z}_j) - \mathbf{F}(\omega_0, \mathbf{Z}_j)}{t_j} \\
&\geq L(\omega_0; v).
\end{aligned}$$

Combining with (2), we showed that the limit exists and is equal to $L(\omega_0; v)$. \square

Since the function $f(\omega)$ is a differentiable continuous function on a convex set, the first-order necessary condition of local minima is a standard result in optimization.

Theorem 12. *If ω_\star is a local minimizer of $f(\omega)$ over Θ , then for any feasible direction $v \in \mathbb{R}^{kn}$ at ω_\star ,*

$$Df(\omega_\star; v) \geq 0.$$

4 Numerical Experiments

We experimentally evaluate and compare performance of the various persistence diagram representations in the k -means algorithm by simulation. We remark that our experimental setup differs from those conducted by Marchese *et al.* (2017), who compare their clustering to other non-persistence-based machine learning clustering algorithms; we are interested in the performance of the k -means algorithm in the context of persistent homology.

Specifically, we implement the k -means clustering algorithms on vectorized persistence diagrams: in the spirit of machine learning, many embedding methods have been proposed for persistence diagrams so that existing statistical methods and machine learning algorithms can then be applied to these vectorized representations; we systematically compare the performance of k -means on three of the most popular embeddings. We also implement k -means on persistence diagrams themselves as well as persistence measures, which requires adapting the algorithm to comprise the respective metrics as well as the appropriate means. In total, we study a total of five representations for persistent homology in the k -means algorithm: three are embeddings of persistence diagrams, persistence diagrams themselves, and finally, their generalization to persistence measures.

4.1 Embedding Persistence Diagrams

The algebraic topological construction of persistence diagrams results in a highly nonlinear data structure where existing statistical and machine learning methods cannot be applied. The problem of embedding persistence diagrams has been extensively researched in TDA, with many proposals for vectorizations of persistence diagrams. In this paper, we study three of the most commonly-used persistence diagram embeddings and their performance in the k -means clustering algorithm: Betti curves; persistence landscapes (Bubenik, 2015); and persistence images (Adams *et al.*, 2017). These vectorized persistence diagrams can then be directly applied to the original k -means algorithm.

The Betti curve of a persistence diagram D is a function that takes any $z \in \mathbb{R}$ and returns the number of points (x, y) in D , counted with multiplicity, such that $z \in [x, y)$. Figure 2a shows an example of a persistence diagram and its corresponding Betti curve is shown in Figure 2b. It is a simplification of the persistence diagram, where information on the persistence of the points is lost. The Betti curve takes the form of a vector by sampling values from the function at regular intervals.

Persistence landscapes as functional summaries of persistence diagrams were introduced by Bubenik (2015) with the aim of integrability into statistical methodology. The persistence landscape is a set of functions $\{\lambda_k\}_{k \in \mathbb{N}}$ where $\lambda_k(t)$ is the k th largest value of

$$\max \left(0, \min_{(x,y) \in D} (t - x, y - t) \right).$$

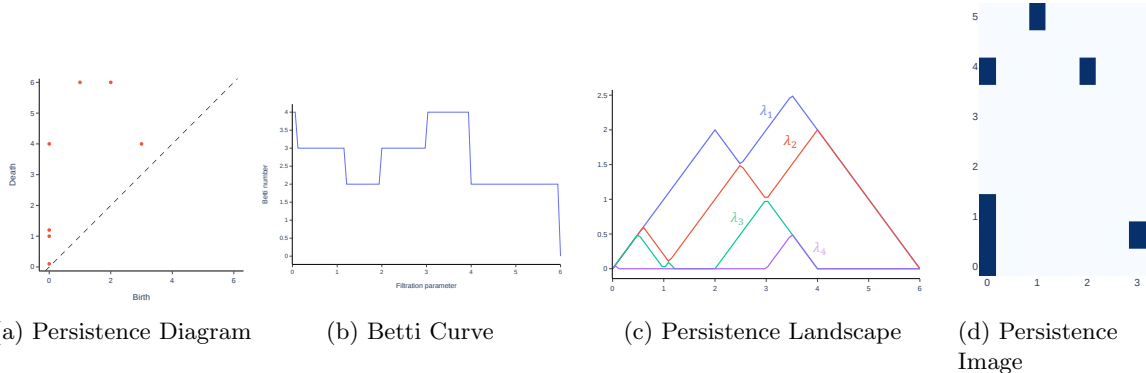


Figure 2: Representations of Persistent Homology.

Figure 2c continues the example of the persistence diagram in Figure 2a and shows its persistence landscape. The construction of the persistence landscape vector is identical to that of the Betti curve, but for multiple λ functions for one persistence diagram.

The persistence image introduced by Adams *et al.* (2017) is 2-dimensional representation of a persistence diagram as a collection of pixel values, shown in Figure 2d. The persistence image is obtained from a persistence diagram by discretizing its *persistence surface*, which is a weighted sum of probability distributions. The original construction by Adams *et al.* (2017) uses Gaussians, which are also used in this paper. The pixel values are concatenated row by row to form a single vector representing one persistence diagram. The persistence image is the only representation we study that lies in Euclidean space; Betti curves and persistence landscapes are functions and therefore lie in function space.

4.2 Simulation Study

The generated datasets are equipped with known labels; therefore any clustering output can be compared to these labels using the Adjusted Rand Index (ARI)—a performance metric where a score of 1 suggests perfect alignment of clustering output and true labels, and 0 suggests random clustering (Hubert & Arabie (1985)).

We simulated 3-dimensional point clouds sampled from 3 classes from the surfaces of common topological shapes; circles, spheres and tori. We vary the noise in this dataset by adding random displacement to sampled points to study the change in algorithm performance as the complexity of the data increases. Table 1a shows the results of k -means clustering with 3 clusters on the five persistent homology representations of the simulated dataset.

Tables 1b and 1c show the average results from 100 repetitions comparing the persistence landscapes and persistence images, and the persistence diagrams and persistence measures, respectively. We see that persistence measures outperform persistence diagrams with consistently higher scores on average. Among the embedded persistence diagrams, the persistence landscapes produced the best clustering results, followed by the persistence images, and finally the Betti curves, which were not able to cluster accurately for any level of noise.

Software and Data Availability

The code used to perform all experiments is publicly available at the GitHub repository <https://github.com/pruskileung/PH-kmeans>.

5 Discussion

In this paper, we studied the k -means clustering algorithm in the context of persistent homology. We studied the subtleties of the convergence of the k -means algorithm in persistence diagram space and in the Karush–

Noise	PL	PI	BC	PD	PM
0.0	1.0	1.0	1.0	1.0	1.0
1.0	1.0	0.898	0.052	1.0	1.0
2.0	0.898	1.0	0.043	1.0	1.0
3.0	0.898	0.731	0.202	1.0	1.0
4.0	1.0	1.0	0.416	1.0	1.0
5.0	0.717	0.898	0.266	1.0	1.0
10.0	0.667	0.423	0.225	1.0	0.898

(a) Clustering results for simulated data

Noise	Mean PL score	Mean PI score
1.0	0.998 (0.012)	0.892 (0.063)
2.0	0.974 (0.037)	0.965 (0.036)
3.0	0.911 (0.082)	0.922 (0.105)
4.0	0.89 (0.085)	0.852 (0.161)
5.0	0.843 (0.112)	0.734 (0.186)
10.0	0.633 (0.088)	0.453 (0.014)

(b) Performance of PLs vs PIs in 100 repetitions of the simulated data

Noise	Mean PD score	Mean PM score
1.0	0.971 (0.202)	0.996 (0.020)
2.0	0.952 (0.260)	0.961 (0.069)
3.0	0.892 (0.251)	0.947 (0.064)
4.0	0.904 (0.218)	0.946 (0.074)
5.0	0.890 (0.220)	0.945 (0.070)
10.0	0.854 (0.185)	0.892 (0.077)

(c) Clustering results for simulated data using PDs and PMs

Kuhn–Tucker framework, which is a nontrivial problem given the highly nonlinear geometry of persistence diagram space. Specifically, we showed that the solution to the optimization problem is a partial optimal point, Karush–Kuhn–Tucker point, as well as a local minimum. These results refine, generalize, and extend that of Marchese *et al.* (2017), who show convergence to a partial optimal point, which need not be a local minimum. Experimentally, we studied and compared the performance of the algorithm for inputs of three embedded persistence diagrams and modified the algorithm for inputs of persistence diagrams themselves as well as their generalizations to persistence measures. We found that empirically, clustering results on persistence diagrams and persistence measures directly were better than on vectorized persistence diagrams, suggesting a loss of structural information in the most popular persistence diagram embeddings.

Our results inspire new directions for future studies, such as other theoretical aspects of k -means clustering in the persistence diagram and persistence measure setting, such as convergence to the “correct” clustering as the input persistence diagrams and persistence measures grow; and other properties of the algorithm such as convexity, other local or global optimizers, and analysis of the cost function. The problem of information preservation in persistence embedding has been previously studied where statistically, an embedding based on tropical geometry results in no loss of statistical information via the concept of sufficiency (Monod *et al.*, 2019). Additional studies from the perspective of entropy would facilitate a better understanding and quantification of the information lost in embedding persistence diagrams that negatively affect the k -means algorithm. This in turn would inspire more accurate persistence diagram embeddings for machine learning.

Acknowledgments

We wish to thank Antonio Rieser for helpful discussions. We also wish to acknowledge the Information and Communication Technologies resources at Imperial College London for their computing resources which were used to implement the experiments in this paper.

References

- ADAMS, HENRY, EMERSON, TEGAN, KIRBY, MICHAEL, NEVILLE, RACHEL, PETERSON, CHRIS, SHIPMAN, PATRICK, CHEPUSHTANOVA, SOFYA, HANSON, ERIC, MOTTA, FRANCIS, & ZIEGELMEIER, LORI. 2017. Persistence images: A stable vector representation of persistent homology. *Journal of Machine Learning Research*, **18**.
- ARTHUR, DAVID, & VASSILVITSKII, SERGEI. 2006. *k-means++: The Advantages of Careful Seeding*. Technical Report 2006-13. Stanford InfoLab.
- BUBENIK, PETER. 2015. Statistical Topological Data Analysis using Persistence Landscapes. *Journal of Machine Learning Research*, **16**, 77–102.
- CAO, LEI, MCLAREN, DARIAN, & PLOSKER, SARAH. 2022. Centrosymmetric stochastic matrices. *Linear and Multilinear Algebra*, **70**(3), 449–464.
- CHAZAL, FRÉDÉRIC, DE SILVA, VIN, GLISSE, MARC, & OUDOT, STEVE. 2016. *The structure and stability of persistence modules*. Springer.
- DIVOL, VINCENT, & CHAZAL, FRÉDÉRIC. 2019. The density of expected persistence diagrams and its kernel based estimation. *Journal of Computational Geometry*, **10**(2), 127–153.
- DIVOL, VINCENT, & LACOMBE, THÉO. 2021a. Estimation and quantization of expected persistence diagrams. *International Conference on Machine Learning*, 2760–2770.
- DIVOL, VINCENT, & LACOMBE, THÉO. 2021b. Understanding the topology and the geometry of the space of persistence diagrams via optimal partial transport. *Journal of Applied and Computational Topology*, **5**(1), 1–53.
- HARTIGAN, J. A., & WONG, M. A. 1979. Algorithm AS 136: A *k*-Means Clustering Algorithm. *Applied Statistics*, **28**(1), 100.
- HUBERT, LAWRENCE, & ARABIE, PHIPPS. 1985. Comparing partitions. *Journal of Classification*, **2**(1), 193–218.
- ISLAMBEKOV, UMAR, & GEL, YULIA R. 2019. Unsupervised spacetime clustering using persistent homology. *Environmetrics*, **30**(4), e2539.
- MAJUMDAR, SOURAV, & LAHA, ARNAB KUMAR. 2020. Clustering and classification of time series using topological data analysis with applications to finance. *Expert Systems with Applications*, **162**, 113868.
- MARCHESE, ANDREW, MAROULAS, VASILEIOS, & MIKE, JOSH. 2017. *K*-means clustering on the space of persistence diagrams. *Wavelets and Sparsity XVII*, **10394**, 103940W.
- MILEYKO, YURIY, MUKHERJEE, SAYAN, & HARER, JOHN. 2011. Probability measures on the space of persistence diagrams. *Inverse Problems*, **27**(12), 124007.
- MONOD, ANTHEA, KALIŠNIK, SARA, PATINO-GALINDO, JUAN ÁNGEL, & CRAWFORD, LORIN. 2019. Tropical Sufficient Statistics for Persistent Homology. *SIAM Journal on Applied Algebra and Geometry*, **3**(2), 337–371.
- PANAGOPOULOS, DIMITRIOS. 2022. Topological data analysis and clustering. *arXiv preprint arXiv:2201.09054*.
- SELIM, SHOKRI Z, & ISMAIL, MOHAMED A. 1984. K-means-type algorithms: A generalized convergence theorem and characterization of local optimality. *IEEE Transactions on pattern analysis and machine intelligence*, 81–87.
- TURNER, KATHARINE, MILEYKO, YURIY, MUKHERJEE, SAYAN, & HARER, JOHN. 2014. Fréchet means for distributions of persistence diagrams. *Discrete & Computational Geometry*, **52**(1), 44–70.